Nonlinear Dyn (2025) 113:17289–17309
https://doi.org/10.1007/s11071-025-11006-5

RESEARCH

Numerical investigation of an SIR fractional order delay epidemic model in the framework of Mittag–Leffler kernel

Bashir Al-Hdaibat · Mahmoud H. DarAssi · Irfan Ahmad · Muhammad Altaf Khan · Reem Algethamie · Ebraheem Alzahrani

Received: 10 January 2025 / Accepted: 13 February 2025 / Published online: 1 March 2025

Abstract A fractional order delay SIR model in Mittag–Leffler kernel is proposed. The model initially presented in integer order system and later extended by applying the Atangana-Baleanu derivative. The essential properties of the model are investigated. Equilibrium points of the fractional system are analyzed, and multiple equilibrium points are identified and discussed. The permanence of the model for $\mathcal{R}_0 \leq 1$ is established. Local stability of the fractional model is examined. For the fractional system, we prove the existence and uniqueness (EUs) result. We obtain the numerical results for fractional delay system by presenting a novel computational procedure, and various sets of numerical values are used to generate graphical results. Different solution behaviors of the model are observed for various numerical values and fractional order parameters.

Keywords Delay model · Permanence · Stability results · Numerical scheme · Discussion

B. Al-Hdaibat
Department of Mathematics, Faculty of Science, The Hashemite University, Zarqa, Jordan

M. H. DarAssi
Department of Basic Sciences, Princess Sumaya University for Technology, Amman 11941, Jordan

I. Ahmad
Department of Clinical Laboratory Sciences, College of Applied Medical Science, King Khalid University, 61421 Abha, Saudi Arabia

M. A. Khan
Faculty of Natural and Agricultural Sciences, University of the Free State, Bloemfontein 9300, South Africa

M. A. Khan (✉)
School of Health and Environmental Science, Korea University, Seoul 02841, South Korea
e-mail: altafdir@gmail.com; muhammadaltafkhan@korea.ac.kr

M. A. Khan
Laboratory of Vaccine and Biomolecules, Institute of Bioscience, Universiti Putra Malaysia, 43400, UPM Serdang Selangor, Malaysia

R. Algethamie
Department of Mathematics, Faculty of Science, Al-Baha University, 65799 Alaqiq, Saudi Arabia

E. Alzahrani
Department of Mathematics, Faculty of Science, King Abdulaziz University, P.O. Box 80203, 21589 Jeddah, Saudi Arabia

1 Introduction

The comprehension of disease control and eradication is a primary objective of mathematical epidemiology [1]. In order to examine ecological and epidemiological phenomena, mathematical models are frequently utilized, see [2]. For example, to investigate the plant disease dynamics a mathematical model with detailed results is provided in [2]. Mathematical compartmental models are frequently used to illustrate how infectious illnesses propagate throughout a community. In this way, there are several subclasses within the overall population under study. The entire population is split into three groups in this instance: susceptible, infectious,

and recovered or removed, which are often represented by the letters S, I, and R. It is stated that the sickness condition of this group determines its structures [3]. An epidemic disease model in SIR type that addresses the contacts among healthy and infected people to estimate the ill individuals in community within a specific time frame. A mathematical model in the form of an SIR model considered in [4] for the disease spread among humans and vector. Therefore, it is reasonable to suppose that after an individual infects a susceptible vector, a delay period exists while the infectious agents develop within the vector before it is capable of transmitting the infection. Delays in time have been identified as causing system instability [5]. Several authors considered the time delays and the distributed delays in their work, see [6–8], which proved that the incubation is harmful for the stability and asymptotic analysis of the model. The smoking model in Mittag–Leffler kernel has been investigated in [9]. A fractional derivative approach in the modeling of Hepatitis B is presented in [10].

From the past decades, researchers have taken keen interest in FDs to model and simulate mathematical models that arise from various fields of science and engineering. Under different kernels, researchers have constructed and analyzed mathematical models in application domains. The Atangana-Baleanu [11], generalized cardinal sine kernel [12], and Caputo-Fabrizio [13] etc., are examples of FDs with non-singular kernel classes. FDs are classified mainly into two categories, i. e., the class of singular kernel that includes Caputo type and the Riemann-Liouville (RL) fractional differential equations [14–16]. Because FD operators are non-local, and serve as an effective and convenient mathematical tool by addressing real life problems depending on memory effects, they allow for a more reasonable representation of complex behaviors. Many research works have been presented in the literature to study the dynamics and solution of the fractional order systems [17–21]. For example, the authors in [17] constructed differential mathematical models in singular and non-singular kernels by providing effective numerical schemes for their numerical solution. In [18], the authors investigated the dynamics of Lassa fever to understand its dynamics in fractional derivative. In [19], a fractional system for diabetes has been constructed to obtain the solution in Caputo case. The authors in [20] used the fractional derivative to understand the drug resistance in the facilitation survival model. The COVID-19 outbreaks and their impact of on vaccination has been considered in [21] in terms of fractional order model. To study cancer dynamics in the framework of the MIttag–Leffler kernel, a mathematical model has been proposed in [22].

In the recent past, many FD models with non-singular kernel have been considered in various applications in fractional calculus. Specifically, it has been found that the FD model with Mittag–Leffler (ML) under Atangana-Baleanu derivative (ABD) is appropriate for characterizing a wide range of complicated real life problems. In fractional order models, the Mittag–Leffler (ML) functions arise naturally as a solution to the fractional differential equations (FDEs). FDEs are the generalization of the integer order system by incorporating the memory effects, which shows the nonlinear behavior of the model. The ML functions are used often to describe processes with long time memory while the model with traditional derivative relies on assumptions of "instantaneous" responses. The ML kernel allows for gradual or delayed reactions which are essential in complex biological systems, such as anomalous diffusion, and long term dependencies. Biological models, such as immune response and disease latency, exhibit memory effects, where current state depends on the past events. This includes delayed reactions, such as immune response or disease incubation periods which cannot be captured by integer order models. The ML kernel FDs are used to describe real-world challenges which fail to comply with the power-law. They have all the characteristics of fractional operators that include a power-law kernel, including non-locality and non-singularity. FDs with ML kernels have been used extensively and suitably to describe a number of fractional calculus applications; for example, see [23–26]. The authors in [23] considered the ML kernel by presenting some novel properties associated with fractional derivatives. A class of FDDEs to provide the existence and uniqueness results has been presented in [24]. The application of the ML kernel to the modeling of mpox infection has been considered in [25]. The authors in [26], considered the fractional derivative approach for the solution of financial system under the variable demand elasticity.

The models in fractional calculus that appeared usually are the fractional delay differential equation (FDDE), which is a differential equation that combines FDs with temporal delays. Differential systems containing FDs and delays can be used to precisely articulate the real life problems relying on time delays and

memory effects, which reflect the influence of previous states on the present situation. FDDEs are considered highly effective tool to handle real world problem that contain history in various areas such signal processing, population dynamics, ecology, psychology, control theory, and neural networks. Regarding the existence and achieving the unique solution associated with FDDEs, this can be seen in the work of [24,27–29]. Consequently, computational techniques have been suggested to resolve these models, as exemplified by references [30–32]. Nonetheless, the majority of FDDEs that have been explored follows that power law-kernel and FD Caputo derivative [24,27–32]. For example, the linear FDDEs with multiple delays has been considered in [27] to present the associated the result associated to it. An FDDEs model have been used by the authors in [28] to provide the bifurcation and stability results. Nth order FDDEs with multiple terms have been explored by the authors in [29] by establishing the stability and existing of solution. An operational matrix approach to handle numerically the FDDEs has been explored in [30]. The numerical solution of FDDEs by considering the generalized Adams technique is given in [31]. FFDEs with higher order numerical approaches has been presented in [32].

In this work, we consider a time delay model and present its analysis in the framework of FDDEs. Presenting in Section 2, the definition ad integral, which makes the foundation for the proposed problem. Construction of the model and their associated properties are respectively discussed in Section 3, and 4. In Sections 5, and 6 discuss the stability analysis, as well as the existence of solution and their uniqueness. The numerical scheme and its graphical results are given in Sections 7 and 8 respectively. The summary of the results is shown in Section 9.

2 Fractional derivatives involve Mittag–Leffler(ML)

We present some related definitions of FDs involving ML kernels. In [11], the authors introduced an ML based FDs defined by:

Definition 1 ([11]) Suppose $\eta \in (0,1)$, $b > 0$, and $g \in B^1(0,b)$, the FD in ML form of g of order η is described as, for $t \in (0,b)$:

$$D_t^{\eta} g(t) = \frac{\mathcal{B}(\eta)}{1-\eta} \int_0^t E_{\eta}(-\psi_{\eta}(t-\tau)^{\eta}) g'(\tau) d\tau, \quad (1)$$

where $\psi_{\eta} = \eta/(1-\eta)$, and $\mathcal{B}(0) = \mathcal{B}(1) = 1$, defines the normalization function. Whereas E_{η} is ML function for $\eta > 0$, and $x \in C$,

$$E_{\eta} = \sum_{j=0}^{\infty} \frac{x^j}{\Gamma(\eta j + 1)},$$

and $B^1(0,b) = \{\overline{g} \in C^1[0,b] | \, \overline{g}' \in L'(0,b)\}$.

Definition 2 [11] Suppose $\eta \in (0,1)$, $b > 0$ and $g \in L'(0,b)$, then the fractional integral associated with ML FD of g order η described as, for $t \in (0,b)$:

$$I^{\eta} g(t) = \mathcal{A}_1 g(t) + \mathcal{A}_2 \int_0^t (t-\tau)^{\eta-1} f(\tau) d\tau,$$

where $\mathcal{A}_1 = \frac{(1-\eta)}{B(\eta)}$, and $\mathcal{A}_2 = \frac{\eta}{B(\eta)\Gamma(\eta)}$.

3 Mathematical model

An SIR epidemic model incorporating disease transmission with an incubation period is given within the framework of fractional delay differential equation, considering Mittag–Leffler kernel. Previously, the authors in [3] constructed the model for the integer case in delay differential equations. The host population is categorized into three different groups: The healthy people, $S(t)$, those infected with the disease, $I(t)$, and infectious people who are removed or recovered from an infection, $R(t)$, at any time t. It is assumed that the healthy population $S(t)$, grows according to the logistic growth model, which is characterized by a carrying capacity B, and the intrinsic growth rate b, while the incidence has been used in the model as a bilinear mass action. Models with logistic growth rates describe situations where the population grows rapidly when its size is small, but as it approaches the carrying capacity, then the growth rate decrease due to the available limited resources, eventually stabilizing. Based on the above discussions, we present the model in the following taking from [3]:

$$\begin{cases} \frac{dS}{dt} = -\kappa S(t) I(t-\tau) + b\left(1 - \frac{S(t)}{B}\right) S(t), \\ \frac{dI}{dt} = \kappa S(t) I(t-\tau) - (d_1 + \delta) I(t), \\ \frac{dR}{dt} = \delta I(t) - d_2 R(t), \end{cases} \quad (2)$$

where $\tau > 0$ represents the incubation time, κ is the average number of interactions per infected individual per unit time, and d_1 and d_2 respectively denote the natural mortality rate of the infected people and recovered

individuals. The parameters given in the system (2) are positive. Now, we nondimensionalize the system (2) using the relation,

$$\overline{S} = \frac{S}{B},\ \overline{I} = \frac{I}{B},\ \overline{R} = \frac{R}{B},\ \overline{t} = t\kappa B,\ \overline{b} = \frac{b}{\kappa B},$$
$$\overline{d}_1 = \frac{d_1}{\kappa B},\ \overline{d}_2 = \frac{d_2}{\kappa B},\ \overline{\delta} = \frac{\delta}{\kappa B}.$$

Then, the system (2) reduces to the following when dropping the 'bar':

$$\begin{cases} \frac{dS}{dt} = -S(t)I(t-\tau) + b(1-S(t))S(t), \\ \frac{dI}{dt} = S(t)I(t-\tau) - (d_1+\delta)I(t), \\ \frac{dR}{dt} = \delta I(t) - d_2 R(t), \end{cases} \tag{3}$$

The initial conditions (ICs) $\psi = (\psi_1, \psi_2, \psi_3)$ of the system (3) in the Banach space can be defined as follows:

$$C_+ = \Big\{\psi \in C([-\tau, 0] \in \mathbb{R}^3_+) : \psi_1(\pi) = S(\pi),$$
$$\psi_2(\pi) = I(\pi),\ \psi_3(\pi) = R(\pi)\Big\},$$

where $\mathbb{R}^3_+ = \{(S, I, R) \in \mathbb{R}^3 : S \geq 0, I \geq 0, R \geq 0\}$. From a biological point of view, it is assumed that $\psi_j(0) > 0$, for $j = 1, 2, 3$. Then, we extend the system (3) to the fractional delay differential equation follows the ABD established for the FDEs given by,

$$\begin{cases} D_t^\eta S(t) = -S(t)I(t-\tau) + b(1-S(t))S(t), \\ D_t^\eta I(t) = S(t)I(t-\tau) - (d_1+\delta)I(t), \\ D_t^\eta R(t) = \delta I(t) - d_2 R(t), \end{cases} \tag{4}$$

where η is the fractional order.

4 Basics of the model

Solutions boundedness

Assume that $X(t) = S(t) + I(t) + R(t)$, then the time differentiations of $X(t)$, and the use of equations (4), we get

$$\begin{aligned} D_t^\eta X &= b(1-S)S - d_1 I - d_2 R, \\ &\leq bS - d_1 I - d_2 R, \\ &\leq S(b+1) - S - d_1 I - d_2 R, \\ &\leq Z(b+1) - dX, \end{aligned}$$

where $d = \min\{d_1, d_2, 1\}$. The use of integration on the above equation [33], leads to the following solutions

$$X(t) \leq \frac{Z}{d}(b+1) + \Big(\frac{-Z}{d}(b+1) + X(0)\Big)E_\eta(-dt^\eta),$$

where E_η is the ML function. We get $0 \leq X(t) \leq (Z/d)(b+1)$ when t tends ∞. So, the feasible solution associated to system (4) enter the region

$$\Gamma = \Big\{(S, I, R) \in [0, 1]^3 : X \leq \frac{Z}{d}(b+1) + \epsilon,\ \forall \epsilon > 0\Big\}. \tag{5}$$

4.1 Analysis of the equilibrium points

The following three equilibrium points, namely $\mathcal{D}_0$, $\mathcal{D}_1$, and $\mathcal{D}_2$ exists for system (4), that is

(i) A trivial equilibrium exists, $\mathcal{D}_0 = (0, 0, 0)$.
(ii) DFE equilibrium exists, $\mathcal{D}_1 = (1, 0, 0)$.
(iii) A positive endemic equilibrium exists, $\mathcal{D}_2$, given by

$$\mathcal{D}_2 = (S^*, I^*, R^*) = \Big(\delta + d_1,\ b\,(\delta + d_1)$$
$$(1 - \mathcal{R}_0),\ \frac{b\delta(\mathcal{R}_0 - 1)(d+\delta)}{d_2}\Big),$$

where $\mathcal{R}_0 = \frac{1}{d_1+\delta}$.

4.2 Permanence

Theorem 1 *If $\mathcal{R}_0 \leq 1$, then the system (4) solutions Γ for any ϵ holds $(S(t), I(t), R(t)) \to (1, 0, 0)$ for t approaches ∞.*

Proof Define a Lyapunov function,

$$L(t) = I(t) + g_1 R(t) + g_2 \int_{t-\tau}^{t} I(\psi)d\psi + \frac{g_3}{2}(S(t) - 1)^2, \tag{6}$$

where $g_j > 0$, for $j = 1, 2, 3$. Then, differentiating of (6) with t, using model (4), we have

$$\begin{aligned} D_t^\eta L(t) &= D_t^\eta I(t) + g_1 D_t^\eta R(t) + g_2[I(t) \\ &\quad - I(t-\tau)] + g_3(S(t) - 1)D_t^\eta S(t), \\ &= S(t)I(t-\tau) - (d_1+\delta)I(t) \\ &\quad + g_1[\delta I(t) - d_2 R(t)] \\ &\quad + g_2[I(t) - I(t-\tau)] \\ &\quad + g_3(S(t) - 1)[-S(t)I(t-\tau) \\ &\quad + b(1 - S(t))S(t)], \\ &= [S(t) - g_2 + g_3 S(t)(1 - S(t))]I(t-\tau) \\ &\quad + [-(d_1+\delta) + g_1\delta + g_2]I(t) \\ &\quad - g_1 d_2 R(t) - g_3 b S(t)(1 - S(t))^2, \end{aligned}$$

$$= [S(t) - g_2 + g_3 S(t)(1 - S(t))]I(t-\tau) + \left[g_1\delta + g_2 - \frac{1}{\mathcal{R}_0}\right]I(t) - g_1 d_2 R(t) - g_3 b S(t)(1-S(t))^2. \quad (7)$$

Now choosing $g_j > 0$ for $j = 1, 2, 3$ that satisfy,

$$g_1\delta + g_2 < \frac{1}{\mathcal{R}_0}, \text{ and } (1+g_3)^2 < 4g_2g_3, \quad (8)$$

then $D_t^\eta L(t) \leq 0$. Since, $\mathcal{D}_0$ is unstable, $D_t^\eta L(t) = 0$ is equivalent to $S = 0$, $I = 0$, $R = 0$, then the maximum invariant set in $\{(S, I, R) \in \Gamma : D_t^\eta L(t) = 0\}$ is the $\mathcal{D}_1$, which is the singleton set. Then, the Lyapunov LaSalle's theorem shows that $(S(t), I(t), R(t)) \to (1, 0, 0)$ when $\mathcal{R}_0 < 1$ for $t \to \infty$. From condition (8), it is possible that $g_2 > 1$,similarly, we can write the second condition $g_3^2 + 2(1-2g_2)g_3 + 1 < 0$, that can be true if $g_3 > 0$ if $(1-2g_2) < 0$, and $(1-2g_2)^2 > 1$. For the case when $\mathcal{R}_0 = 1$, implies that $d_1 + \delta = 1$. Since $S'(t) \leq b(1 - S(t))S(t)$, $S(t)$ is decreasing always with above 1. If it is below 1 then it must be below 1 strictly for all the times. With this two cases arises, $S(t)$ approves unity when $t \to \infty$, and there exists T such that $S(t)$ less than unity for all $t > T$. In first case it is to show that $I(t)$ approaches 0. We integrate the first equation of the model (4) and obtain

$$\begin{aligned} S(t+\tau) - S(\tau) &= -\int_\tau^{t+\tau} S(v)I(v-\tau)dv + \int_\tau^{t+\tau} b(1-S(v))S(v)dv, \\ &\leq -\int_\tau^{t+\tau} I(v-\tau)dv + \int_\tau^{t+\tau} b(1-S(v))S(v)dv, \\ &\leq -\int_0^{t} I(v)dv + \int_\tau^{t+\tau} b(1-S(v))S(v)dv. \end{aligned}$$

So,

$$\int_0^t I(v)dv \leq \int_\tau^{t+\tau} b(1-S(v))S(v)dv - S(t+\tau) + S(\tau) \leq S(\tau) \leq S(0).$$

When $t \to \infty$, we get $I(t) \to 0$ and $I(t) \in L^1(0, \infty)$. To get the result for the second case, let

$$V(t) = I(t) + \int_{t-\tau}^t I(v)dv.$$

Then for every $t > T + \tau$,

$$\begin{aligned} V'(t) &= I'(t) + I(t) - I(t-\tau) \\ &= (S(t) - 1)I(t-\tau) < 0. \end{aligned}$$

Follows the result given in [34], we prove $\lim_{t\to\infty} I(t) = 0$. We have from equation third of the model (3), that $\lim_{t\to\infty} I(t) = 0$ implies $\lim_{t\to\infty} R(t) = 0$. Which proven that $\lim_{t\to\infty}(S(t), I(t), R(t)) \to (1, 0, 0)$ when $\mathcal{R}_0 \leq 1$. □

5 Local stability

The local asymptotical stability (LAS) of the equilibrium pointss associated to the model (4) shall be discussed in the present part. Consider a general Jacobian matrix of the system (4) at $\mathcal{D} = (\overline{S}, \overline{I}, \overline{R})$:

$$\overline{J} = \begin{bmatrix} -\overline{I} + b - 2b\overline{S} - \lambda & -\overline{S}e^{-\lambda\tau} & 0 \\ \overline{I} & \overline{S}e^{-\lambda\tau} - (d_1+\delta) - \lambda & 0 \\ 0 & \delta & -d_2 - \lambda \end{bmatrix}. \quad (9)$$

The Jacobian $\overline{J}$ at $\mathcal{D}_0$ has the characteristics equation

$$(\lambda - b)(\lambda + d_2)(\lambda + d_1 + \delta) = 0. \quad (10)$$

One of the root of the equation (10) has a positive root, that is $\lambda = b$, that makes $\mathcal{D}_0$ unstable. At $\mathcal{D}_1$, we have the characteristics equations,

$$(\lambda + b)(\lambda + d_2)(\delta + d_1 + e^{-\lambda\tau} + \lambda) = 0. \quad (11)$$

The two roots of (11) has negative real parts, that is $\lambda = -b$, $\lambda = -d_2$ and root of

$$G(\lambda) = \delta + d_1 - e^{-\lambda\tau} + \lambda = 0, \quad (12)$$

when $\tau = 0$, we have $\lambda = 1 - (\delta + d_1) = 1 - \frac{1}{\mathcal{R}_0} < 0$ if $\mathcal{R}_0 < 1$. If $\lambda = i\theta$ is the solution of equation (12), then it becomes,

$$\theta^2 + (d_1+\delta)^2 = 1 = \theta^2 + \frac{1}{\mathcal{R}_0^2},$$

implies that θ has a negative roots, and hence $G(\lambda)$ has roots that contain negative real parts which makes $\mathcal{D}_1$ LAS. If $\mathcal{R}_0 = 1$, then $\lambda = 1 - (d_1 + \delta) = 1 - \frac{1}{\mathcal{R}_0} = 0$ is the root of (12). To determine other roots, we take $\lambda = \alpha + i\theta$, then we have

$$\alpha + i\theta + d_1 + \delta - \exp(-(\alpha + i\theta)) = 0, \quad (13)$$

and further simplifying, when $\mathcal{R}_0 = 1$, we get $(\alpha + 1)^2 + \theta^2 = \exp(-\alpha\tau)$. For $\alpha \leq 0$ it is sure that $\mathcal{D}_1$ is linearly neutrally stable.

6 EU result of the fractional system

We present the EU results associated to the system (4) in this section. To establish the result, we follow the procedure given in [35] that presented to obtained the EU for the epidemic disease model. Here, we provide result for our proposed model, by applying first the integral operator given in (2) on model (4), and obtain the following:

$$\begin{aligned}
S(t) - S(0) &= \mathcal{A}_1 K_1(\mathrm{G}(t)) \\
&\quad + \mathcal{A}_2 \int_0^t (t-\xi)^{\eta-1} K_1(\boldsymbol{G}(\xi))d\xi, \\
I(t) - I(0) &= \mathcal{A}_1 K_2(\mathrm{G}(t)) \\
&\quad + \mathcal{A}_2 \int_0^t (t-\xi)^{\eta-1} K_2(\boldsymbol{G}(\xi))d\xi, \\
R(t) - R(0) &= \mathcal{A}_1 K_3(\boldsymbol{G}(t)) \\
&\quad + \mathcal{A}_2 \int_0^t (t-\xi)^{\eta-1} K_3(\boldsymbol{G}(\xi))d\xi, \quad (14)
\end{aligned}$$

where $\boldsymbol{G}(t) = [S(t), I(t), R(t)]$, and

$$\begin{aligned}
K_1(\boldsymbol{G}(t)) &= -S(t)I(t-\tau) + b(1-S(t))S(t), \\
K_2(\boldsymbol{G}(t)) &= = S(t)I(t-\tau) - (d_1+\delta)I(t), \\
K_3(\boldsymbol{G}(t)) &= = \delta I(t) - d_2 R(t).
\end{aligned}$$

Let $K(\boldsymbol{G}(t)) = [K_1(G(t)), K_2(G(t)), K_3(G(t))]$, and $\boldsymbol{G}_0 = [S(0), I(0), R(0)]$, then we can expressed equation (14) in the following way,

$$\begin{aligned}
\boldsymbol{G}(t) - \boldsymbol{G}_0 &= \mathcal{A}_1 K(\boldsymbol{G}(t)) \\
&\quad + \mathcal{A}_2 \int_0^t (t-\xi)^{\eta-1} K(\boldsymbol{G}(\xi))d\xi. \quad (15)
\end{aligned}$$

The iterative process leads to

$$\begin{aligned}
\boldsymbol{G}_n(t) - \boldsymbol{G}_0 &= \mathcal{A}_1 K(\boldsymbol{G}_{n-1}(t)) \\
&\quad + \mathcal{A}_2 \int_0^t (t-\xi)^{\eta-1} K(\boldsymbol{G}_{n-1}(\xi))d\xi, \\
\boldsymbol{G}_0(t) &= \boldsymbol{G}_0. \quad (16)
\end{aligned}$$

From equations (15) and (16), we get

$$\begin{aligned}
\boldsymbol{G}_n(t) - \boldsymbol{G}_{n-1}(t) &= \mathcal{A}_1\Big[K(\boldsymbol{G}_{n-1}(t)) - K(\boldsymbol{G}_{n-2}(t))\Big] \\
&\quad + \mathcal{A}_2 \int_0^t (t-\xi)^{\eta-1} [K(\boldsymbol{G}_{n-1}(\xi)) \\
&\quad - K(\boldsymbol{G}_{n-2}(\xi))]d\xi. \quad (17)
\end{aligned}$$

Let $\Delta_n(t) = \boldsymbol{G}_n(t) - \boldsymbol{G}_{n-1}(t)$, and so $\boldsymbol{G}_n(t) = \sum_{i=0}^{n} \Delta_i(t)$. So, we have

$$\begin{aligned}
\|\Delta_n(t)\| &= \Big\|\mathcal{A}_1\Big[K(\boldsymbol{G}_{n-1}(t)) - K(\boldsymbol{G}_{n-2}(t))\Big] \\
&\quad + \mathcal{A}_2 \int_0^t (t-\xi)^{\eta-1} [K(\boldsymbol{G}_{n-1}(\xi)) \\
&\quad - K(\boldsymbol{G}_{n-2}(\xi))]d\xi\Big\|, \\
&\leq \mathcal{A}_1 \Big\|K(\boldsymbol{G}_{n-1}(t)) - K(\boldsymbol{G}_{n-2}(t))\Big\| \\
&\quad + \mathcal{A}_2 \int_0^t (t-\xi)^{\eta-1} \Big\|K(\boldsymbol{G}_{n-1}(\xi)) \\
&\quad - K(\boldsymbol{G}_{n-2}(\xi))\Big\|d\xi. \quad (18)
\end{aligned}$$

When K satisfy Lipschitz condition with respect to G, then

$$\begin{aligned}
\|\Delta_n(t)\| &\leq \mathcal{A}_1 L \Big\|\boldsymbol{G}_{n-1}(t) - \boldsymbol{G}_{n-2}(t)\Big\| \\
&\quad + \mathcal{A}_2 L \int_0^t (t-\xi)^{\eta-1} \\
&\quad \times \Big\|\boldsymbol{G}_{n-1}(t) - \boldsymbol{G}_{n-2}(t)\Big\|d\xi, \\
&= \mathcal{A}_1 L \Big\|\Delta_{n-1}(t)\Big\| \\
&\quad + L\mathcal{A}_2 \int_0^t (t-\xi)^{\eta-1} \Big\|\Delta_{n-1}(t)]\Big\|d\xi. \quad (19)
\end{aligned}$$

Further, we get

$$\|\Delta_n(t)\| \leq \Big(\mathcal{A}_1 L + \frac{\eta L t^{\eta}}{B(\eta)\Gamma(\eta+1)}\Big)^2 \|\Delta_{n-2}(t)\|. \quad (20)$$

Also, we can get

$$\begin{aligned}
\|\Delta_n(t)\| &\leq \Big(\mathcal{A}_1 L + \frac{\eta L t^{\eta}}{B(\eta)\Gamma(\eta+1)}\Big)^n \|\Delta_0(t)\|, \\
&\leq \Big(\mathcal{A}_1 + \frac{\eta t^{\eta}}{B(\eta)\Gamma(\eta+1)}\Big)^n L^n \max_{t_0 \in [0,T]} \boldsymbol{G}_0(t). \quad (21)
\end{aligned}$$

Consider $\boldsymbol{G}(t) = \sum_{i=0}^{n} \Delta_i(t)$, then we define the sequence $\boldsymbol{G}(t) = \boldsymbol{G}_n(t) + \Phi_n(t)$, where $\Phi_n(t) \to 0$ when $t \to \infty$. So,

$$\begin{aligned}
\boldsymbol{G}(t) - \boldsymbol{G}_n(t) &= \mathcal{A}_1 K(\boldsymbol{G}(t) - \Phi_n(t)) \\
&\quad + \mathcal{A}_2 \int_0^t (t-\xi)^{\eta-1} K(\boldsymbol{G}(\xi) - \Phi_n(\xi))d\xi. \quad (22)
\end{aligned}$$

Further, we have

$$\begin{aligned}
&\boldsymbol{G}(t) - \boldsymbol{G}_0 - \mathcal{A}_1 K(\boldsymbol{G}(t) - \Phi_n(t)) \\
&\quad - \mathcal{A}_2 \int_0^t (t-\xi)^{\eta-1} K(\boldsymbol{G}(\xi) - \Phi_n(\xi))\, d\xi \\
&= \Phi_n(t) + \mathcal{A}_1[K(\boldsymbol{G}(t) - \Phi_n(t)) - K(\boldsymbol{G}(t))]
\end{aligned}$$

$$- \mathcal{A}_2 \int_0^t (t-\xi)^{\eta-1}[K(\boldsymbol{G}(\xi)) - \Phi_n(\xi)) - K(\boldsymbol{G}(\xi))]\, d\xi. \tag{23}$$

Taking norm, we get

$$\begin{aligned}
&\|\boldsymbol{G}(t) - \boldsymbol{G}_0 - \mathcal{A}_1 K(\boldsymbol{G}(t)) \\
&\quad + \mathcal{A}_2 \int_0^t (t-\xi)^{\eta-1} K(\boldsymbol{G}(\xi))\, d\xi\| \\
&\leq \|\Phi_n(t)\| + \mathcal{A}_1 \|K(\boldsymbol{G}(t) - \Phi_n(\xi)) - K(\boldsymbol{G}(\xi))\| \\
&\quad + \mathcal{A}_2 \int_0^t (t-\xi)^{\eta-1} \|K(\boldsymbol{G}(\xi)) \\
&\quad - \Phi_n(\xi)) - K(\boldsymbol{G}(\xi))\|\, d\xi \\
&\leq \|\Phi_n(t)\| + \mathcal{A}_1 L \|\Phi_{n-1}(t)\| \\
&\quad + \frac{\eta t^\eta}{B(\eta)\Gamma(\eta+1)} L \|\Phi_{n-1}(t)\|.
\end{aligned} \tag{24}$$

Equation (24) leads to the following when $n \to \infty$

$$\begin{aligned}
\boldsymbol{G}(t) - \boldsymbol{G}_0 &= \mathcal{A}_1 K(\boldsymbol{G}(t)) \\
&\quad + \mathcal{A}_2 \int_0^t (t-\xi)^{\eta-1} K(\boldsymbol{G}(\xi)) d\xi,
\end{aligned}$$

which completes the proof.

6.1 Uniqueness of solution

We prove the uniqueness of the model (4) by considering that there exists two solutions namely, $\boldsymbol{G}(t)$, and $\boldsymbol{H}(t)$, then we can write

$$\begin{aligned}
\|\boldsymbol{G}(t) - \boldsymbol{H}(t)\| &\leq \mathcal{A}_1 L \|\boldsymbol{G}(t) - \boldsymbol{H}(t)\| \\
&\quad + \frac{\eta t^\eta L}{B(\eta)\Gamma(\eta+1)} \|\boldsymbol{G}(t) - \boldsymbol{H}(t)\|, \\
&\leq \left(\mathcal{A}_1 L + \frac{\eta t^\eta L}{B(\eta)\Gamma(\eta+1)}\right) \\
&\quad \times \|\boldsymbol{G}(t) - \boldsymbol{H}(t)\|.
\end{aligned} \tag{25}$$

Taking n times, we get

$$\begin{aligned}
\|\boldsymbol{G}(t) - \boldsymbol{H}(t)\| &\leq \left(\mathcal{A}_1 L + \frac{\eta t^\eta L}{B(\eta)\Gamma(\eta+1)}\right)^n \\
&\quad \times \|\boldsymbol{G}(t) - \boldsymbol{H}(t)\|.
\end{aligned} \tag{26}$$

If $\mathcal{A}_1 L + \frac{\eta t^\eta L}{B(\eta)\Gamma(\eta+1)} < 1$, then $\|\boldsymbol{G}(t) - \boldsymbol{H}(t)\| \leq 0$ implies $\boldsymbol{G}(t) = \boldsymbol{H}(t)$. This shows that the delay fractional system has a a unique solution.

7 Numerical solution

A number predictor-corrector approaches were suggested in the scientific literature for computing IVPs that have Caputo kind problems formulated in FDEs, see [36–39]. The Adams approach for the fractional system established by the authors in [36] has been shown as an among the most successful and correct numerical approaches to deal with IVPs that constructed in FDES under the Caputo derivative. The authors in [12] presented the predictor-corrector numerical approach for the solution involved in IVPs that involve ML FDs. The present scheme that we are going to present in the following is the modification of the method in [16]. A general time delay fractional model can be represented as follows:

$$\begin{cases} D^\eta x(t) = g(t, x(t), x(t-\theta)), & t \in [0, T], \\ x(t) = f(t), & t \in [-\theta, 0], \end{cases} \tag{27}$$

where $0 < \eta < 1$, $\theta > 0$, $T > 0$, and D^η is a ML kind of FD ($D^\eta = {}^{ML} D^\eta$). In integral form the equation (27) can be formulated as:

$$\begin{cases} x(t) = x(0) + {}^{ML} I^\eta g(t, x(t), x(t-\theta)), & t \in [0, T], \\ x(t) = f(t), & t \in [-\theta, 0]. \end{cases} \tag{28}$$

The problem defines a uniform grid over the domain $[-\theta, T]$ with grid points $t_i = ih$, with $i = -m, -m+1, ..., 0, ...n-1, n$. The parameters n, and m are chosen such that the grid spacing satisfies $h = \frac{T}{n} = \frac{\theta}{m}$, where h is the grid spacing. Over the internal $[-\theta, 0]$, the values $x_i = x(t_i)$, for $i = -m, -m+1, ..., 0$ can be organized as $x_i = f(t_i)$. We are now focusing on the interval $[0, T]$ and considering the grid points t_{i+1}, for $i = 0, 1, ..., n-1$, the following is obtained,

$$\begin{aligned}
x(t_{i+1}) &= x(0) + \mathcal{A}_1 g(t_{i+1}, x(t_{i+1}), x(t_{i+1} - \theta)) \\
&\quad + \mathcal{A}_2 \sum_{j=0}^{i} \int_{t_j}^{t_{j+1}} (t_{i+1} - \rho)^{\eta-1} g(\rho, x(\rho), \\
&\quad x(\rho - \theta)) d\rho.
\end{aligned} \tag{29}$$

To obtain the approximation $x_{i+1} \approx x(t_{i+1})$, the procedure mentioned in [12] can be used to get. For obtaining the predictor step, one can consider the trapezoidal rule on (29) for computing the integrals that give the below corrector formula for $i = 0, 1, ..., n-1$,

$$x_{i+1} = x(0) + \mathcal{A}_3 \sum_{j=0}^{i} a_{j,i+1} g\left(t_j, x_j, x_{j-m}\right)$$

$$+ (\mathcal{A}_1 + \mathcal{A}_3)\, g\left(t_{i+1}, x_{i+1}, x_{i+1-m}\right), \tag{30}$$

since $x\left(t_j - \theta\right) = x(jh - mh) \approx x_{j-m}$, where

$$a_{j,i+1} = \begin{cases} i^{\eta+1} - (i-\eta)(i+1)^{\eta}, & \text{if } j = 0, \\ (i-j+2)^{\eta+1} + (i-j)^{\eta+1} & \\ \quad -2(i-j+1)^{\eta+1}, & \text{if } 1 \le j \le i. \end{cases} \tag{31}$$

The scheme, constituting the predictor step, utilizes the Adams-Bashforth fractional method to evaluate the integrals presented in (29). This replace the term x_{i+1} given in equation (30) on the right side with the predictor approximation x_{i+1}^{p}, which is determined as follows for $i = 0, 1, ..., n-1$:

$$\begin{aligned} x_{i+1}^{P} &= x(0) + \mathcal{A}_1 g\left(t_i, x_i, x_{k-M}\right) \\ &\quad + \mathcal{A}_4 \mathcal{A}_5 g\left(t_j, x_j, x_{j-m}\right). \end{aligned} \tag{32}$$

As a result, the numerical scheme developed to compute the approximation $x_{i+1} \approx x(t_{i+1})$ for the solution of the problem (27) in the domain $[0, T]$ can be shown by the formula:

$$\begin{aligned} x_{i+1} &= x(0) + \mathcal{A}_3 \sum_{j=0}^{i} a_{j,i+1} g\left(t_j, x_j, x_{j-m}\right) \\ &\quad + (\mathcal{A}_1 + \mathcal{A}_3) \\ &\quad g\left(t_{i+1}, x_{i+1}^{p}, x_{i+1-m}\right), \end{aligned} \tag{33}$$

where $x_k \approx x(t_i)$, $i = 0, 1, ..., n-1$, and x_{i+1}^{P} represents the predictor value, which can be computed as outlined in (32), incorporating the determination of the weights $a_{j,i+1}$ as specified in equation (31). We implementing the above scheme to solve our problem (3), which are shown by:

$$\begin{aligned} S_{i+1} &= S(0) + \mathcal{A}_3 \sum_{j=0}^{i} a_{j,k+1} \\ &\quad \times g_1\left(t_j, S_j, I_j, R_j, S_{j-m}, I_{j-m}, R_{j-m}\right) \\ &\quad + (\mathcal{A}_1 + \mathcal{A}_3)\, g_1\left(t_{i+1}, S_{i+1}^{p}, I_{i+1}^{p}, R_{i+1}^{p}, \right. \\ &\quad \left. S_{i+1-m}, I_{i+1-m}, R_{i+1-m}\right), \\ I_{i+1} &= I(0) + \mathcal{A}_3 \sum_{j=0}^{i} a_{j,i+1} \\ &\quad \times g_2\left(t_j, S_j, I_j, R_j, S_{j-m}, I_{j-m}, R_{j-m}\right) \\ &\quad + (\mathcal{A}_1 + \mathcal{A}_3)\, g_2\left(t_{i+1}, S_{i+1}^{p}, I_{i+1}^{p}, R_{i+1}^{p}, \right. \\ &\quad \left. S_{i+1-m}, I_{i+1-m}, R_{i+1-m}\right), \\ R_{i+1} &= R(0) + \mathcal{A}_3 \sum_{j=0}^{k} a_{j,i+1} \\ &\quad \times g_3\left(t_j, S_j, I_j, R_j, S_{j-m}, I_{j-m}, R_{j-m}\right) \\ &\quad + (\mathcal{A}_1 + \mathcal{A}_3)\, g_3\left(t_{i+1}, S_{i+1}^{p}, I_{i+1}^{p}, R_{i+1}^{p}, \right. \\ &\quad \left. S_{i+1-m}, I_{i+1-m}, R_{i+1-m}\right), \end{aligned} \tag{34}$$

where S_{i+1}^{P}, I_{i+1}^{P} and R_{i+1}^{P} show the predictor terms given by,

$$\begin{aligned} S_{i+1}^{P} &= S(0) + \mathcal{A}_1 g_1\left(t_i, S_i, I_i, R_i, S_{i-m}, I_{i-m}, R_{i-m}\right) \\ &\quad + \mathcal{A}_4 \mathcal{A}_5 \\ &\quad \times g_1\left(t_j, S_j, I_j, R_j, S_{j-m}, I_{j-m}, R_{j-m}\right), \\ I_{i+1}^{P} &= I(0) + \mathcal{A}_1 g_2\left(t_i, S_i, I_i, R_i, S_{i-m}, I_{i-m}, R_{i-m}\right) \\ &\quad + \mathcal{A}_4 \mathcal{A}_5 \\ &\quad \times g_2\left(t_j, S_j, I_j, R_j, S_{j-m}, I_{j-m}, R_{j-m}\right), \\ R_{i+1}^{P} &= R(0) + \mathcal{A}_1 g_3\left(t_i, S_i, I_i, R_i, S_{i-m}, I_{i-m}, R_{i-m}\right) \\ &\quad + \mathcal{A}_4 \mathcal{A}_5 \\ &\quad \times g_3\left(t_j, S_j, I_j, R_j, S_{j-m}, I_{j-m}, R_{j-M}\right), \end{aligned} \tag{35}$$

and g_1, g_2 and g_3 are the right sides of the model equation (3),

$$\begin{aligned} g_1(t, S, I, R, S_\tau, I_\tau, R_\tau) &= -S(t)I(t-\tau) \\ &\quad + b(1 - S(t))S(t), \\ g_2(t, S, I, R, S_\tau, I_\tau, R_\tau) &= S(t)I(t-\tau) \\ &\quad - (d_1 + \delta)I(t), \\ g_3(t, S, I, R, S_\tau, I_\tau, R_\tau) &= \delta I(t) - d_2 R(t), \end{aligned} \tag{36}$$

where $\mathcal{A}_3 = \frac{\eta}{B(\eta)} \frac{h^\eta}{\Gamma(\eta+2)}$, $\mathcal{A}_4 = \frac{\eta}{B(\eta)} \frac{h^\eta}{\Gamma(\eta+1)}$, and $\mathcal{A}_5 = \sum_{j=0}^{i} [(i+1-j)^\eta - (i-j)^\eta]$.

8 Numerical results

We shall present the numerical solution of the model (4) with the help of numerical scheme mentioned in (33), with the parameter values listed in the following cases:

8.1 Case 1:

For this case, we take the following parameter values: $d_1 = 0.1$, $b = 0.1$, $\delta = 0.1$, $d_2 = 0.1$, $\tau = 1.2$, and consider different values for the fractional order η as $\eta = 1, 0.99, 0.98, 0.97$. The initial conditions for the populations, as per the source [3] are: $S(0) = 0.7$, $I(0) = 0.3$, $R(0) = 0.2$. Graphical results presented in Figs. 1-3 illustrates the present case. Figure 1 illustrates the result when $\eta = 1$, which matches perfectly with

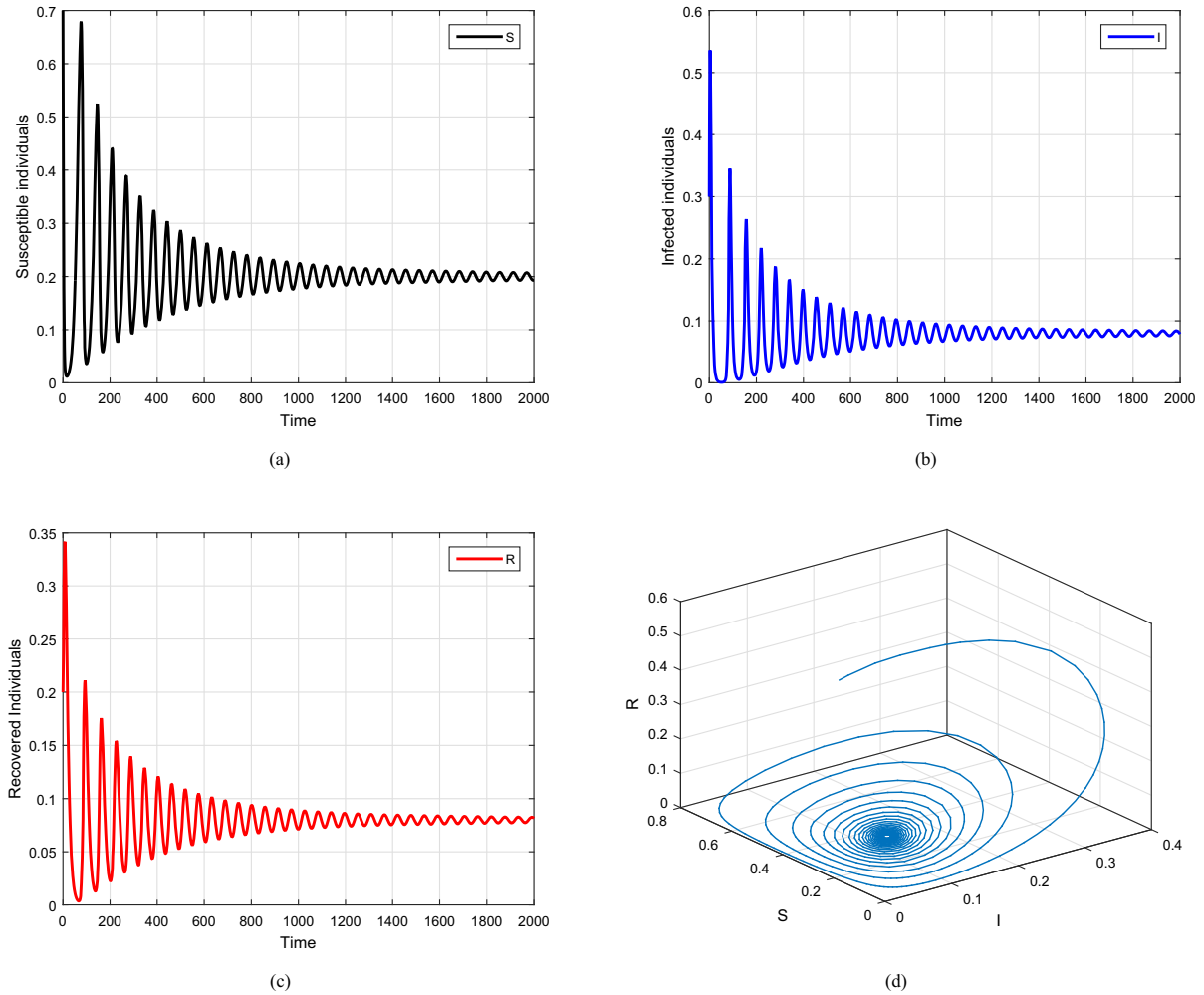

Fig. 1 Graphical results for case 1 of the system (4) when $\eta = 1$, $\tau = 1.2$, and the parameters listed in Case 1, where subplots **a** to **d** are the compartments, S, I, R, and the phase portraits, respectively

the results presented in Figure 1 of [3] for $\tau = 1.2$. The basic reproduction number $\mathcal{R}_0 = 5 > 3$ for the given results indicates that the system approaches to the unique positive endemic equilibrium, denoted by $E_1 = (0, 2, 0.08, 0.08)$. Additionally, Figs. 2 and Fig. 3 display the dynamics of the population of health, infected and recovered people under different values of η, showing the impact of the fractional order on the model's behavior. The phase portraits of the variables are also shown in Fig. 3, providing further insight into the long term behavior of the system. Figure 4 is given to show the dynamics of the model when taking $\eta = 0.08$ for the values given in Case 1. We use $\eta = 1, 0.95, 0.9, 0.85$ to show the result given in Fig. 5 for the values shown in Case 1.

8.2 Case 2:

In Case 2, we consider the parameters values: $d_1 = 0.1$, $\delta = 0.1, d_2 = 0.1, b = 0.1$, and $\tau = 2.5$. The fractional order η takes the values $\eta = 1, 0.99, 0.98, 0.97$. The initial conditions considered for this case are $S(0) = 0.2$, $I(0) = 0.3$, and $R(0) = 0.1$. Graphical results associated to the present case are presented in Figs. 6 and 7. The reproduction number $\mathcal{R}_0 = 5 > 3$ for this case is obtained. Figures 6 and 7 illustrate the population dynamics of the phase portraits, respectively. These results provide an understanding of how the varying fractional order η influences the behavior of the model under different parameter setting. Figure 8 is given to show the dynamics of the model when tak-

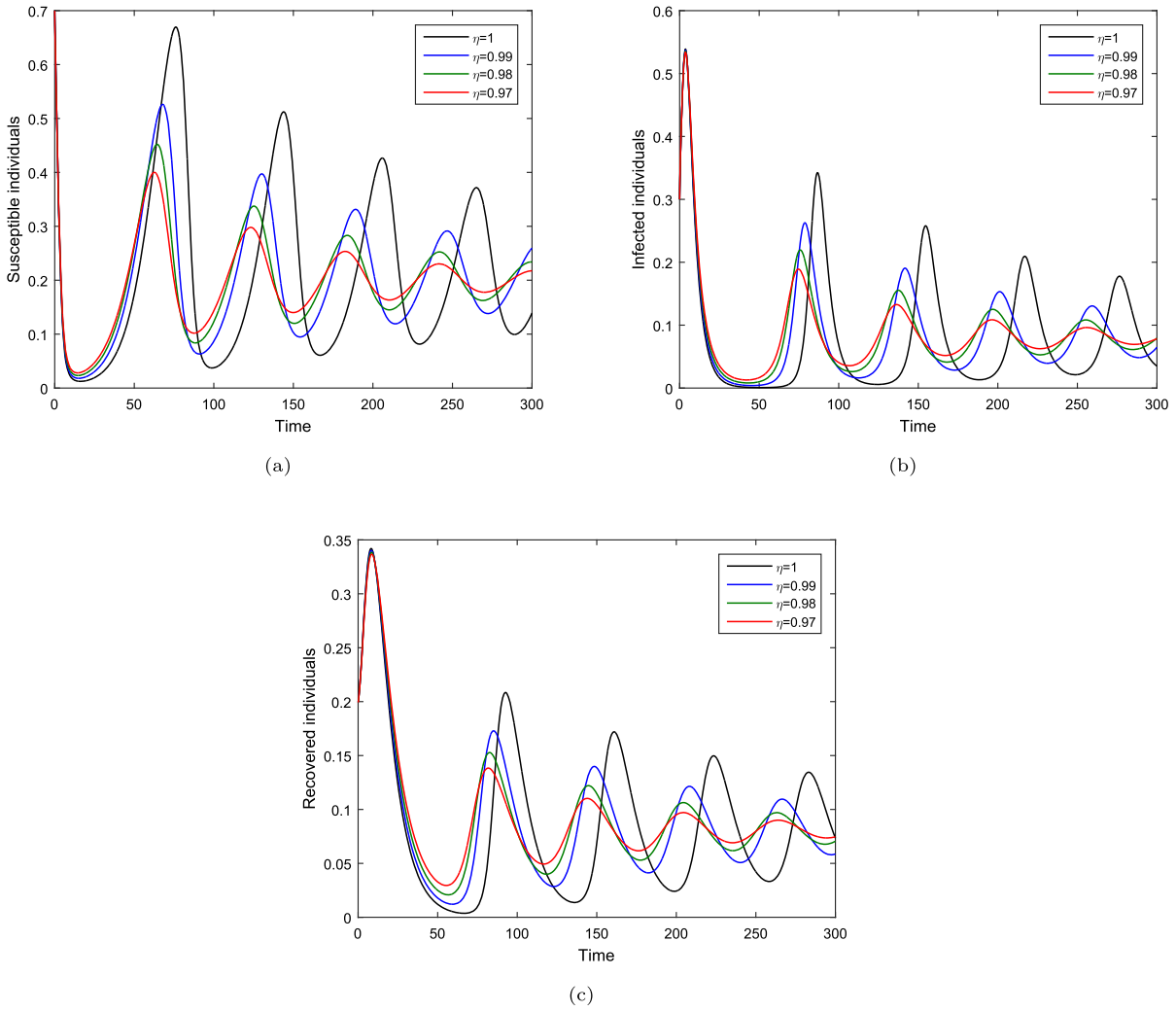

Fig. 2 The plots indicate the simulation of the model (4) with $\tau = 1.2$ and varying $\eta = 1, 0.99, 0.98, 0.97$. Subfigures **a–c** are the dynamics of the populations S, I, R

ing $\eta = 0.08$ for the values given in Case 2, providing different dynamical behavior.

8.3 Case 3:

In Case 3, we use the parameters values: $d_1 = 0.1$, $\delta = 0.4$, $b = 0.1$, $d_2 = 0.1$, and $\tau = 2.5$. We again assign the values to the fractional order η with $\eta = 1, 0.99, 0.98, 0.97$, and consider the initial conditions $S(0) = 0.2$, $I(0) = 0.3$, and $R(0) = 0.2$. The basic reproduction number $\mathcal{R}_0 = 2 < 3$ for the given case has been obtained, indicating that the disease will eradicate from the community in the absence of suitable conditions for endemicity. Figures 9 and 10 present the dynamics of the populations and the respective phase portraits for this case, illustrating the impact of varying η and other parameters on the behavior of the model. Figure 11 is provided to show the dynamics of the model when taking $\eta = 0.08$ for the values given in Case 3.

The graphical results of the fractional delay model with ML kernel highlight the impact of the memory effects and incubation delay on the dynamics of disease. In case 1, when $\tau = 1.2$, and $\eta = 1$, the results match integer order model, while decreasing the value of η shows disease elimination, showing that mem-

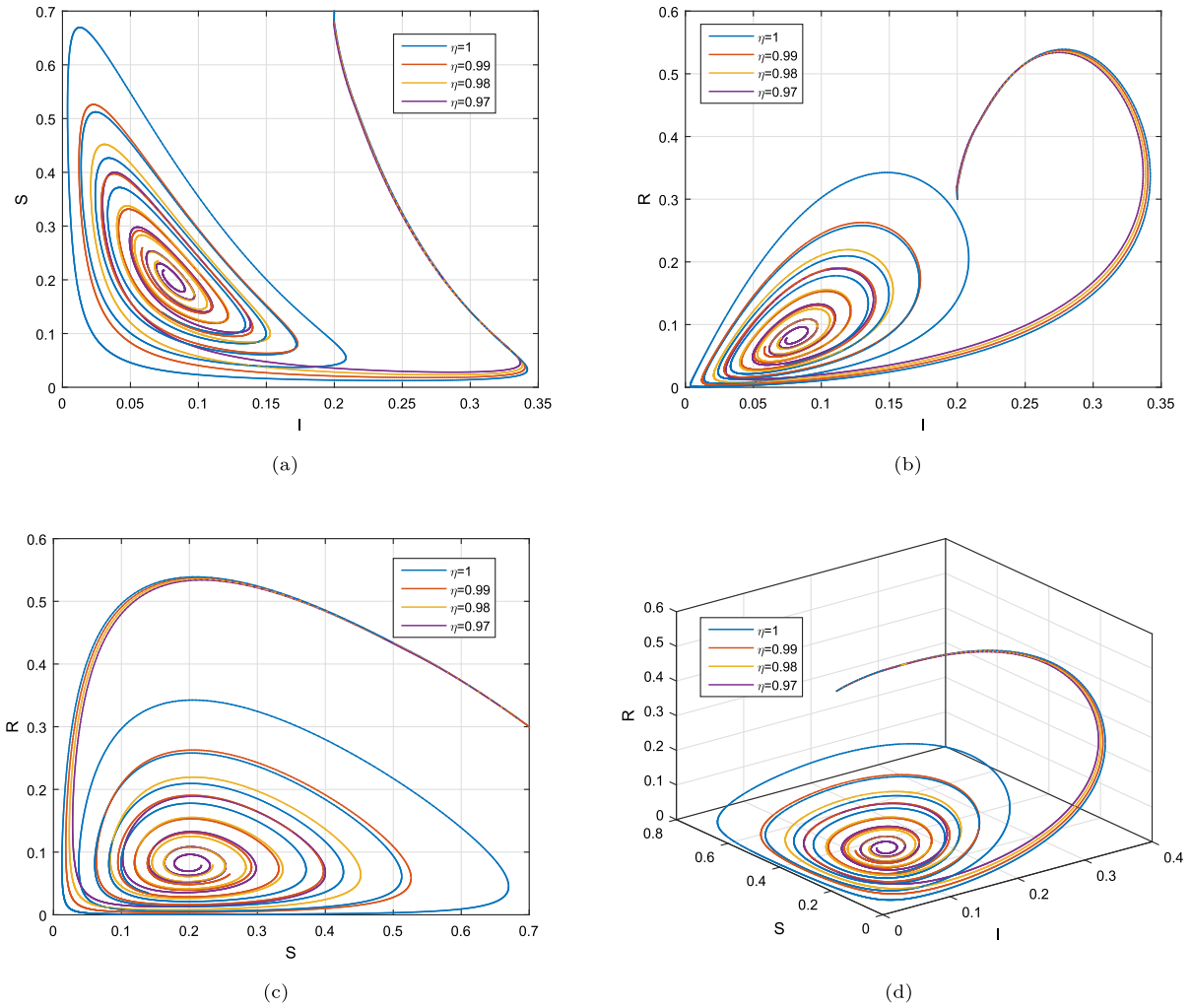

Fig. 3 The plots indicate the simulation of the model (4) with $\tau = 1.2$ and varying $\eta = 1, 0.99, 0.98, 0.97$. Subfigures **a**–**d** are different phase planes of the variables S, I, R

ory effects prolong infection persistence. We can see from case 2, when $\tau = 2.5$ that longer incubation delays cause oscillatory behavior in infection trends, that means that the disease with delay infectiousness require early intervention. Increasing the recovery rate $\delta = 0.4$ given in case 3, the disease reduce more quickly, emphasizing the role of effective treatment and immunity development.

9 Conclusion

In the present analysis, we studied the dynamics of an SIR model under fractional delay differential equation in Mittag–Leffler kernel. Equilibrium points of the model is obtained and have been analyzed. The effects of the incubation time shown by τ on the dynamics of the fractional model have been analyzed. The results indicate that the basic reproduction number and the incubation time determines the disease tendency to the endemic state or its oscillations. The infection dies out for the case $\mathcal{D}_1$ when $\mathcal{R}_0 < 1$, which is globally asymptotically stable. Stability analysis of the equilibrium points $\mathcal{D}_0$, and $\mathcal{D}_1$ for the case τ are considered and discussed. We found that for the case $\mathcal{D}_0$, the model is unstable. For $\mathcal{D}_1$ the model is locally asymptotically stable, and for $\mathcal{R}_0 = 1$, the equilibrium point $\mathcal{D}_1$ is linearly neutrally stable. We obtain the associated result

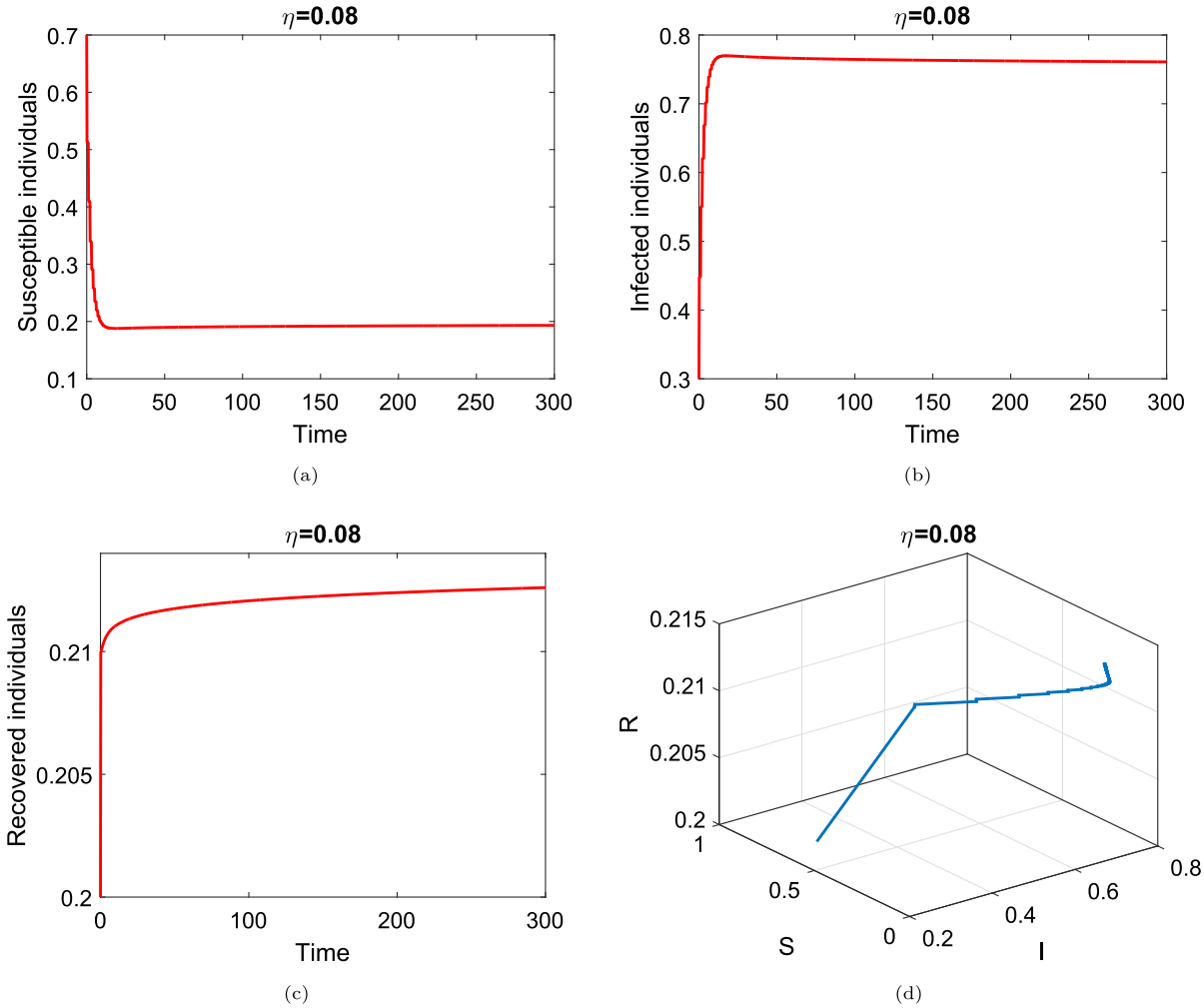

Fig. 4 The plots indicate the simulation of the model (4) for case 1 when $\eta = 0.08$ Sub-figures **a** to **c** are the dynamics of the S, I, and R compartments, while **d** is phase portraits

of EU for the fractional system (4) and discussed with detailed. Numerically solution of the model via new numerical techniques has been presented. We considered different cases to simulate the model. We show that the model for the value of $\tau = 0$ agrees to the original published model. Various values of the delay parameter τ and η are presented and discussed which validated the equilibrium points. When using $\eta = 0.08$, we can observe a compete different behaviors of the model solution.

The present work will be extended to fractional order delay model with stochastic differential in Mittag–Leffler kernel and other fractional operators by comparing the work with the literature. The given model can be extended to fractional order delay optimal control model under stochastic differential equation. Updating to a more complex model with vaccine and other effects with real data in stochastic fractional differential equations will be considered. The present model considered a set of numerical values that are subjected to the present state of the equilibrium points and it may provide different results for different set of parameters values. Further, we use the ABD operator and other operator may provide different results.

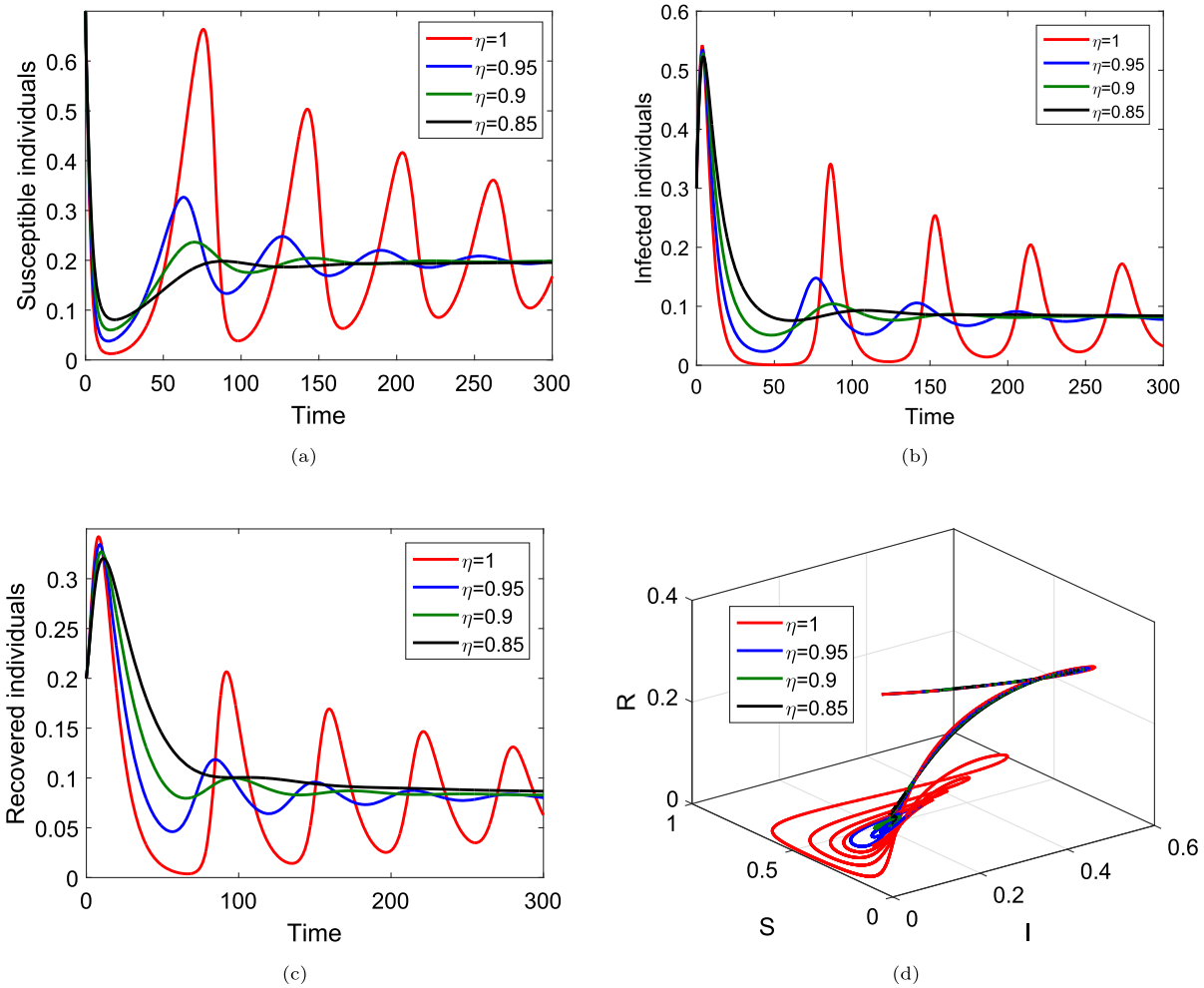

Fig. 5 The plots indicate the simulation of the model (4) for case 1 when $\eta = 1, 0.95, 0.9, 0.85$ Sub-figures **a** to **c** are the dynamics of the S, I, and R compartments, while **d** is the phase portraits

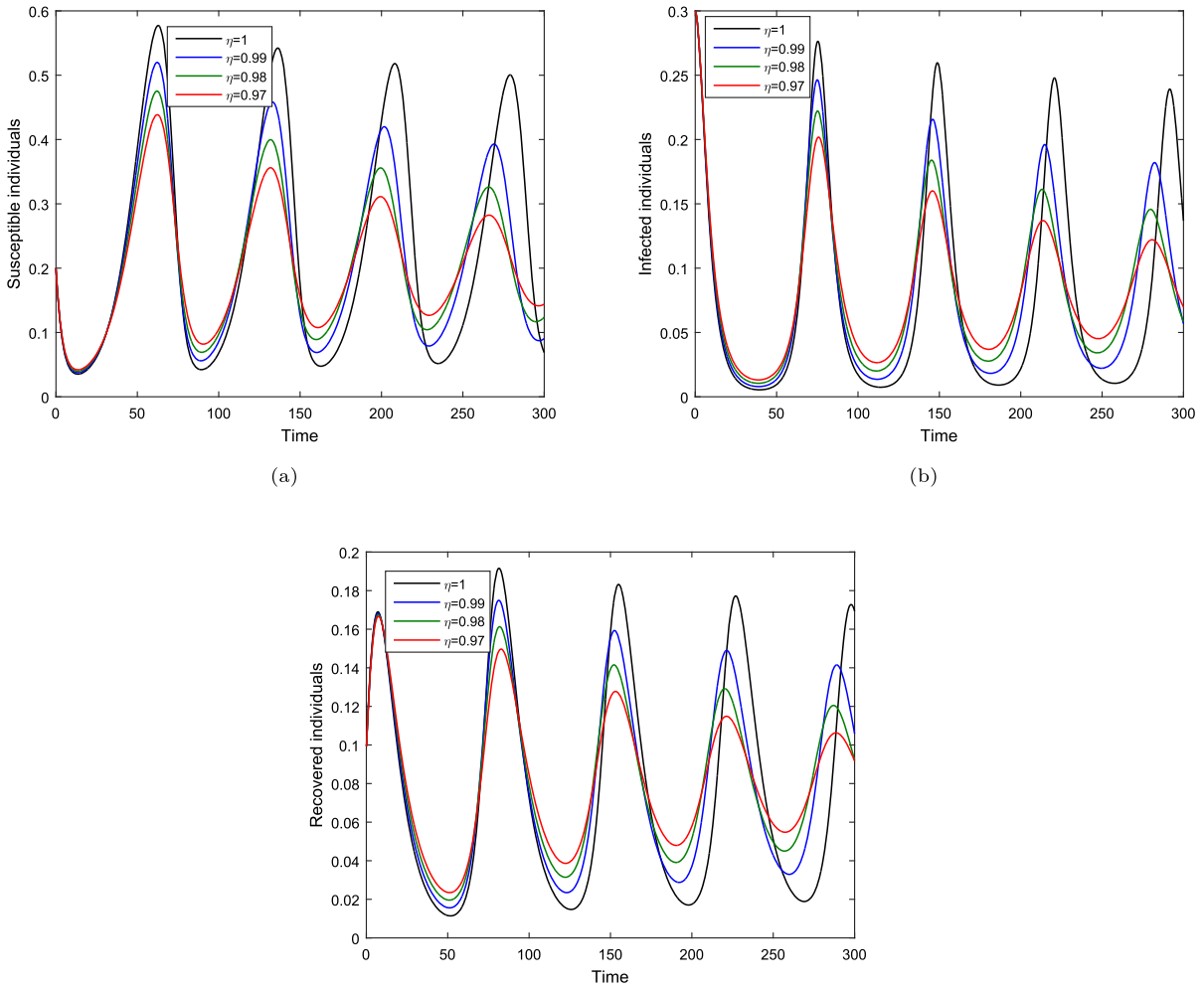

Fig. 6 The plots indicate the simulation of the model (4) when varying $\eta = 1, 0.99, 0.98, 0.97$, and $\tau = 2.5$. Sub-figures **a–c** are the dynamics of the populations S, I, and R

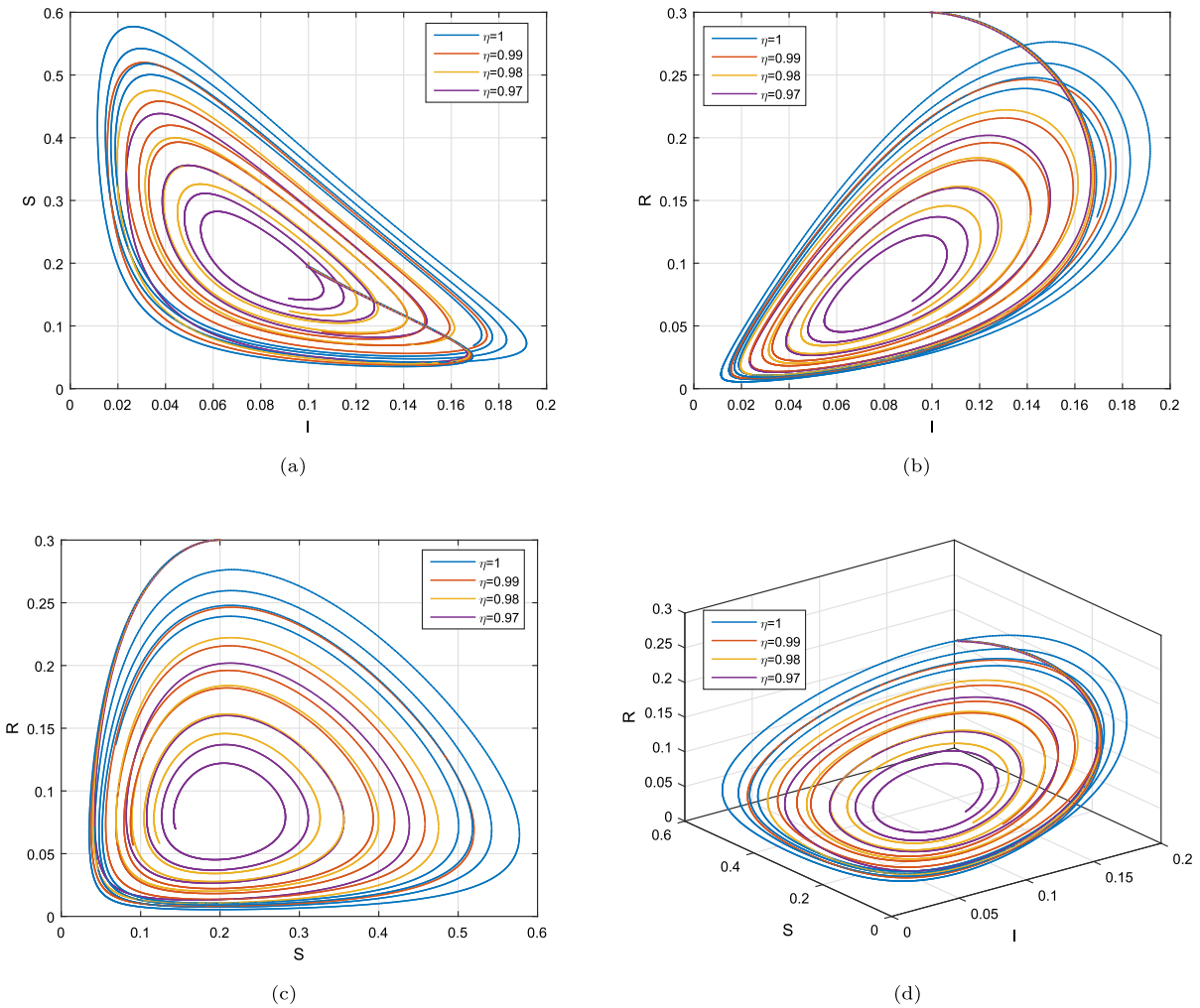

Fig. 7 The plots indicate the simulation of the model (4) when varying $\eta = 1, 0.99, 0.98, 0.97$, and $\tau = 2.5$. Sub-figures **a**-to **c** are the dynamics of the populations S, I, and R

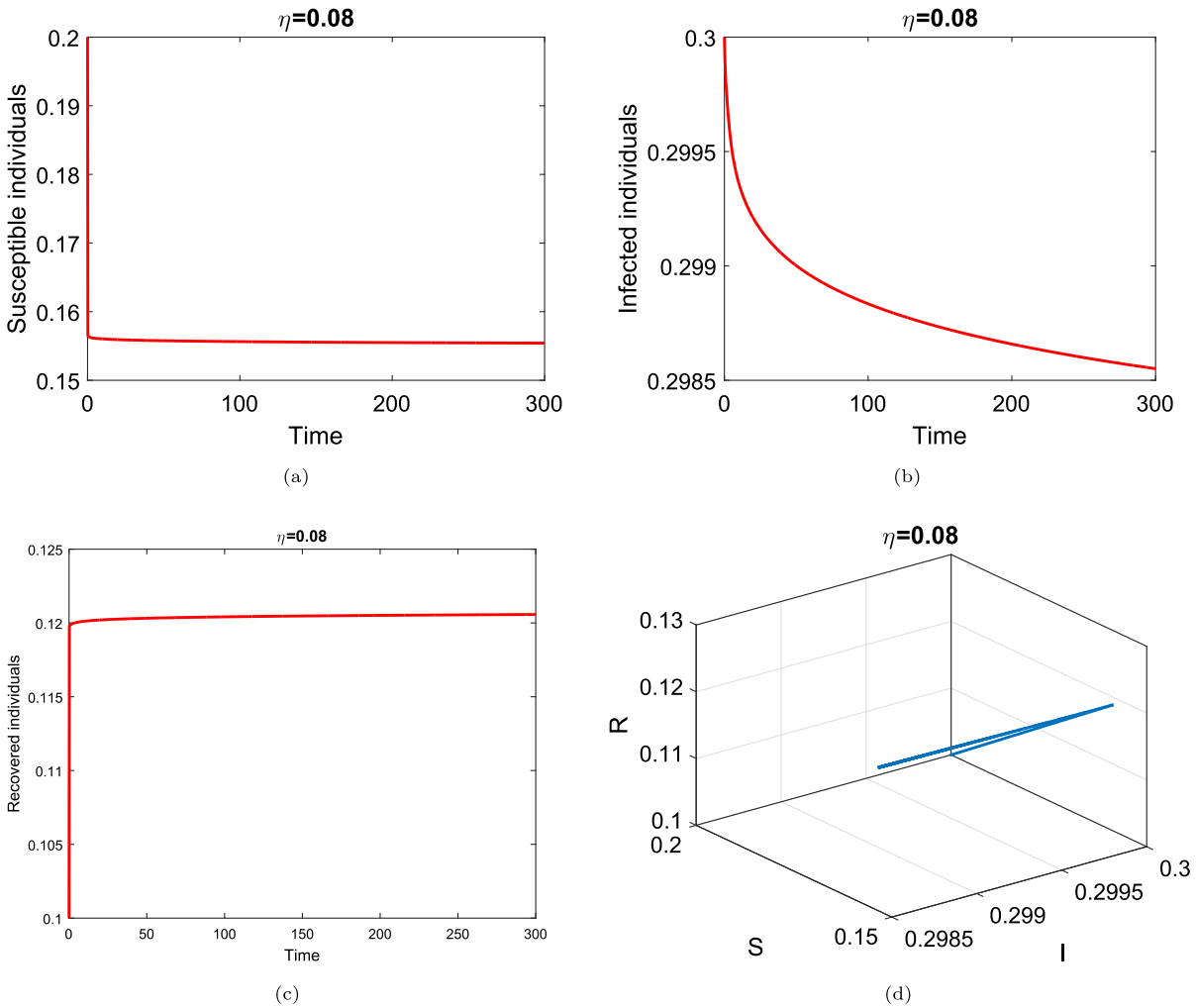

Fig. 8 The plots indicate the simulation of the model (4) for case 2 when $\eta = 0.08$ Sub-figures **a** to **c** are the dynamics of the S, I, and R compartments, while **d** is phase portraits

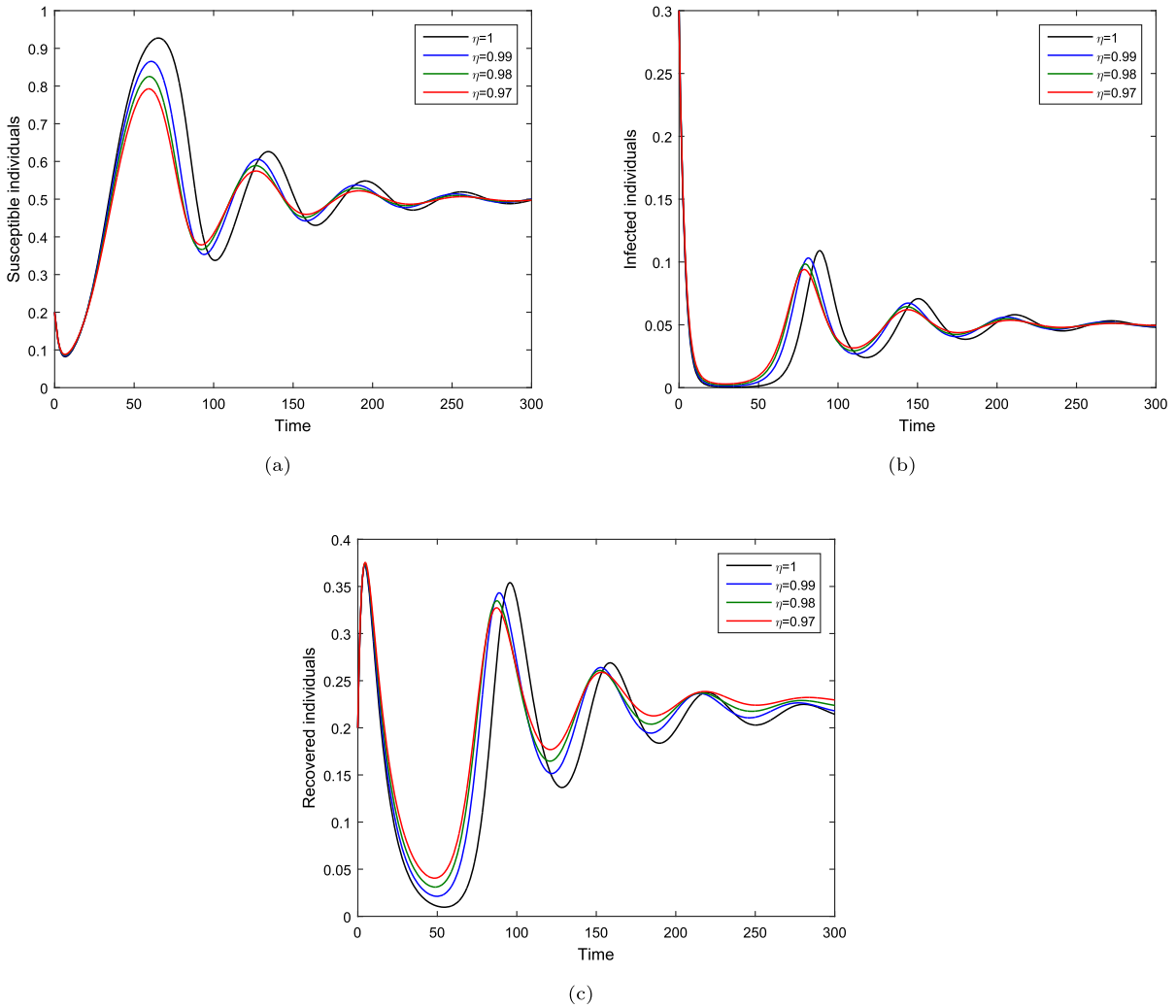

Fig. 9 The plots indicate the simulation of the model (4) when varying $\eta = 1, 0.99, 0.98, 0.97$, $\delta = 0.4$ and $\tau = 2.5$. Sub-figures **a** to **c** are the dynamics of the populations, S, I, and R

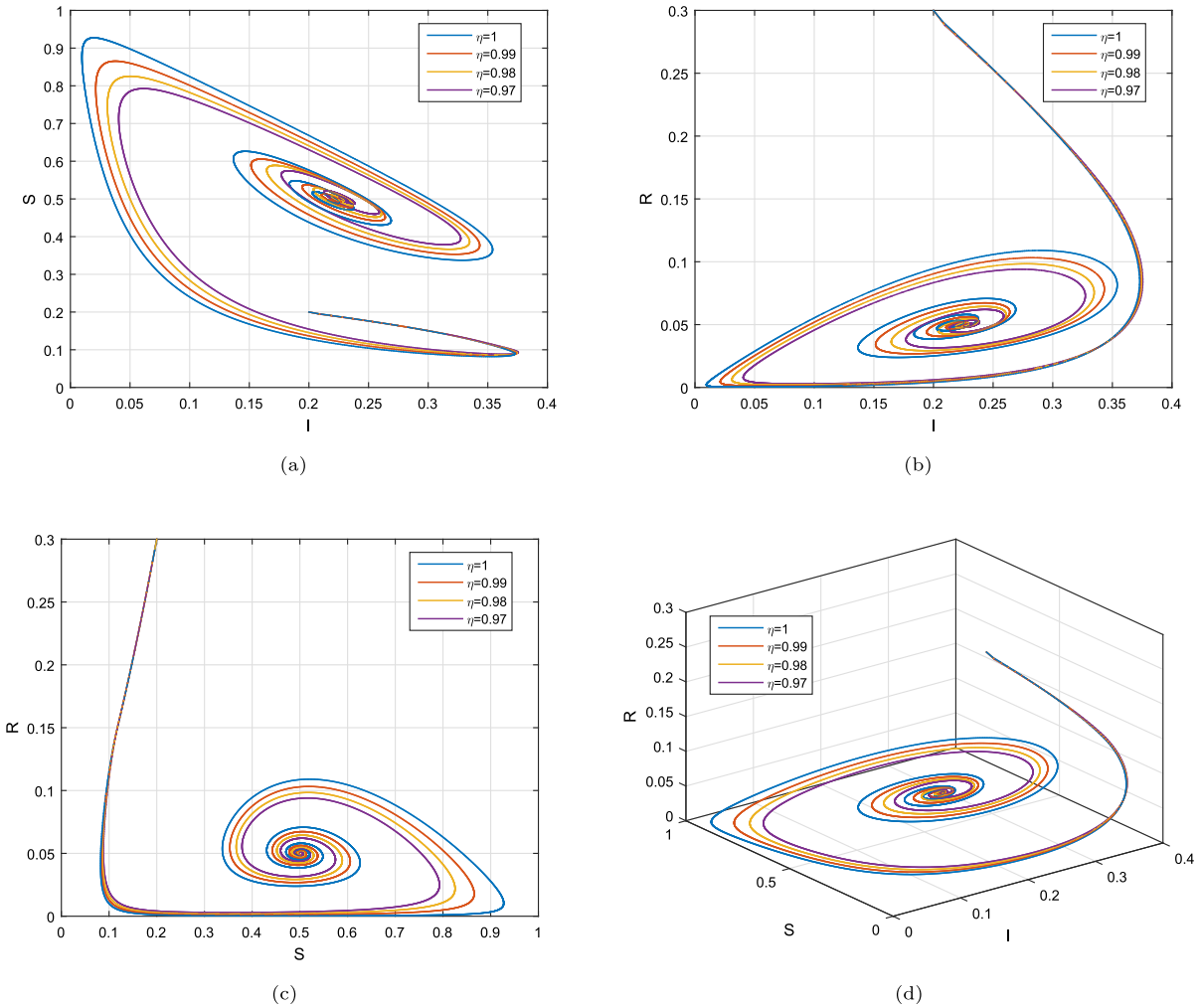

Fig. 10 The plots indicate the simulation of the model (4) when varying $\eta = 1, 0.99, 0.98, 0.97$, $\delta = 0.4$, and $\tau = 2.5$. Sub-figures **a** to **d** are the phase portraits of the variables S, I, and R

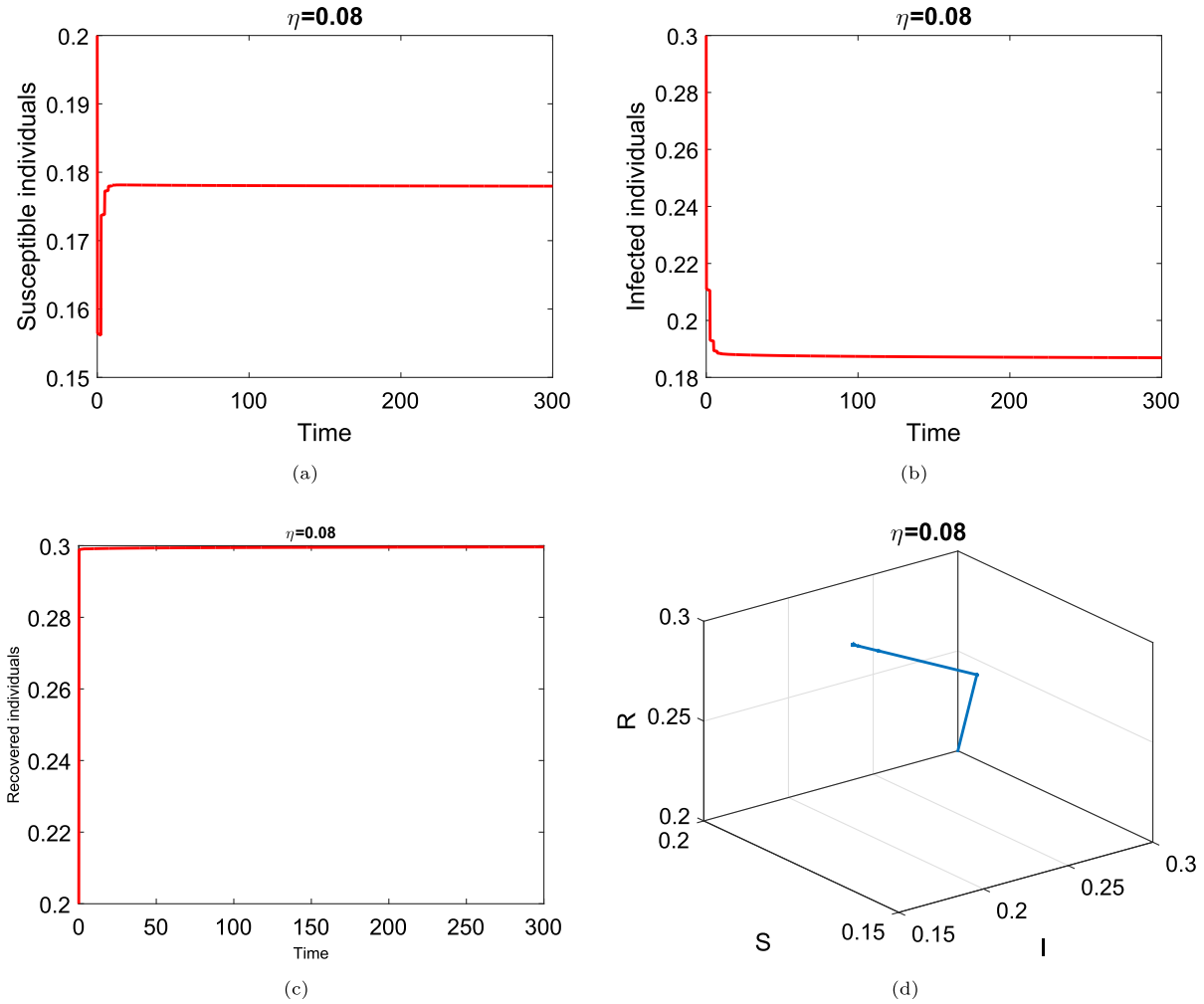

Fig. 11 The plots indicate the simulation of the model (4) for case 3 when $\eta = 0.08$ Sub-figures **a** to **c** are the dynamics of the S, I, and R compartments, while (d) is phase portraits

Acknowledgements The authors are thankful to the Deanship of Research and Graduate Studies, King Khalid University, Abha, Saudi Arabia, for financially supporting this work through the Large Research Group Project under Grant no. R.G.P.2/517/45.

Author contributions All authors equally contributed to this work.

Funding This work was supported by King Khalid University, Abha, Saudi Arabia.

Data availability The data is available from the corresponding author on a reasonable request.

Declarations

Conflict of interest No potential Conflict of interest exists regarding this publications.

References

1. Ma, J., Ma, Z.: Epidemic threshold conditions for seasonally forced seir models. Math.Biosci. Eng. **3**(1), 161–172 (2005)
2. Shabbir, M.S., Din, Q., Sen, M., Gómez-Aguilar, J.: Exploring dynamics of plant-herbivore interactions: bifurcation analysis and chaos control with holling type-ii functional response. J. Math. Biol. **88**(1), 8 (2024)
3. Wang, J.-J., Zhang, J.-Z., Jin, Z.: Analysis of an sir model with bilinear incidence rate. Nonlinear Anal. Real World Appl. **11**(4), 2390–2402 (2010)
4. Cooke, K.L.: Stability analysis for a vector disease model. The Rocky Mountain J. Math. **9**(1), 31–42 (1979)
5. Nakaoka, S., Saito, Y., Takeuchi, Y.: Stability, delay, and chaotic behavior in a lotka-volterra predator-prey system. Math. Biosci. Eng. **3**(1), 173–187 (2005)

6. Beretta, E., Takeuchi, Y.: Global stability of an sir epidemic model with time delays. J. Math. Biol. **33**(3), 250–260 (1995)
7. Takeuchi, Y., Ma, W., Beretta, E.: Global asymptotic properties of a delay sir epidemic model with finite incubation times. Nonlinear Anal.: Theory, Methods Appl. **42**(6), 931–947 (2000)
8. Jin, Z., Ma, Z.: The stability of an sir epidemic model with time delays. Math. Biosci. Eng. **3**(1), 101–109 (2005)
9. Khan, H., Alzabut, J., Gómez-Aguilar, J., Alkhazan, A.: Essential criteria for existence of solution of a modified-abc fractional order smoking model. Ain Shams Eng. J. **15**(5), 102646 (2024)
10. Al-sadi, W., Wei, Z., Abdullah, T.Q., Alkhazzan, A., Gómez-Aguilar, J.: Dynamical and numerical analysis of the hepatitis b virus treatment model through fractal-fractional derivative. Math. Methods Appl. Sci. **48**(1), 639–657 (2025)
11. Atangana, A., Baleanu, D.: New fractional derivatives with nonlocal and non-singular kernel: theory and application to heat transfer model. Therm. Sci. (2016). https://doi.org/10.2298/TSCI160111018A
12. Odibat, Z., Baleanu, D.: A new fractional derivative operator with generalized cardinal sine kernel: numerical simulation. Math. Comput. Simul. **212**, 224–233 (2023)
13. Caputo, M., Fabrizio, M.: A new definition of fractional derivative without singular kernel. Progress in Fract. Diff. Appl. **1**(2), 73–85 (2015)
14. Miller, K.S., Ross, B.: An introduction to the fractional calculus and fractional differential equations. Wiley (1993)
15. Samko, S.G.: Fractional integrals and derivatives. Theory and applications (1993)
16. Kilbas, A.A., Srivastava, H.M., Trujillo, J.J.: Theory and Applications of Fractional Differential Equations. In: North-Holland Mathematics Studies. Elsevier, Amsterdam (2006)
17. Owolabi, K.M., Atangana, A.: Numerical Methods for Fractional Differentiation. In: Studies in Systems Decision and Control. Springer, Cham (2019)
18. Abidemi, A., Owolabi, K.M.: Unravelling the dynamics of lassa fever transmission with nosocomial infections via non-fractional and fractional mathematical models. The Eur. Phys. J. Plus **139**(2), 1–30 (2024)
19. Karaagac, B., Owolabi, K.M., Pindza, E.: A computational technique for the caputo fractal-fractional diabetes mellitus model without genetic factors. Int. J. Dyn. Control **11**(5), 2161–2178 (2023)
20. Shikongo, A., Owolabi, K.M.: On the hindering evolution of drug resistance due to intraspecific competition arising during the facilitation survival for non-genetic resistance with fractal fractional derivative order. Model. Earth Syst. Environ. **9**(2), 2637–2650 (2023)
21. Bhatter, S., Jangid, K., Abidemi, A., Owolabi, K., Purohit, S.: A new fractional mathematical model to study the impact of vaccination on covid-19 outbreaks. Decis. Anal. J. **6**, 100156 (2023)
22. Raza, N., Raza, A., Chahlaoui, Y., Gomez-Aguilar, J.: Numerical analysis of hpv and its association with cervical cancer using atangana-baleanu fractional derivative. Model. Earth Syst. Environ. **11**(1), 60 (2025)
23. Baleanu, D., Fernandez, A.: On some new properties of fractional derivatives with mittag-leffler kernel. Commun. Nonlinear Sci. Numer. Simul. **59**, 444–462 (2018)
24. Wang, F.F., Chen, D.Y., Zhang, X.G., Wu, Y.: The existence and uniqueness theorem of the solution to a class of nonlinear fractional order system with time delay. Appl. Math. Lett. **53**, 45–51 (2016)
25. Khan, M.A., Meetei, M.Z., Shah, K., Abdeljawad, T., Alshahrani, M.Y.: Modeling the monkeypox infection using the mittag-leffler kernel. Open Phys. **21**(1), 20230111 (2023)
26. Lin, X., Wang, Y., Wang, J., Zeng, W.: Dynamic analysis and adaptive modified projective synchronization for systems with atangana-baleanu-caputo derivative: A financial model with nonconstant demand elasticity. Chaos, Solitons Fractals **160**, 112269 (2022)
27. Deng, W., Li, C., Lü, J.: Stability analysis of linear fractional differential system with multiple time delays. Nonlinear Dyn. **48**, 409–416 (2017)
28. Bhalekar, S., Gupta, D.: Stability and bifurcation analysis of a fractional order delay differential equation involving cubic nonlinearity. Chaos, Solitons & Fractals **162**, 112483 (2022)
29. Rahman, G., Agarwal, R.P., Ahmad, D.: Existence and stability analysis of nth order multi term fractional delay differential equation. Chaos, Solitons & Fractals **155**, 111709 (2022)
30. Syam, M.I., Sharadga, M., Hashim, I.: A numerical method for solving fractional delay differential equations based on the operational matrix method. Chaos, Solitons Fractals **147**, 110977 (2021)
31. Zhao, J., Jiang, X., Xu, Y.: Generalized adams method for solving fractional delay differential equations. Math. Comput. Simul. **180**, 401–419 (2021)
32. Gande, N.R., Madduri, H.: Higher order numerical schemes for the solution of fractional delay differential equations. J. Comput. Appl. Math. **402**, 113810 (2022)
33. Li, H.-L., Zhang, L., Hu, C., Jiang, Y.-L., Teng, Z.: Dynamical analysis of a fractional-order predator-prey model incorporating a prey refuge. J. Appl. Math. Comput. **54**, 435–449 (2017)
34. Kuang, Y.: Delay Differential Equations: With Applications in Population Dynamics. In: Mathematics in Science and Engineering. Academic Press, Boston (1993)

35. Ghanbari, B.: A fractional system of delay differential equation with nonsingular kernels in modeling hand-foot-mouth disease. Adv. Difference Equ. **2020**(1), 536 (2020)
36. Diethelm, K., Ford, N.J., Freed, A.D.: A predictor-corrector approach for the numerical solution of fractional differential equations. Nonlinear Dyn. **29**, 3–22 (2002)
37. Deng, W.: Short memory principle and a predictor-corrector approach for fractional differential equations. J. Comput. Appl. Math. **206**(1), 174–188 (2007)
38. Liu, Y., Roberts, J., Yan, Y.: A note on finite difference methods for nonlinear fractional differential equations with non-uniform meshes. Int. J. Comput. Math. **95**(6–7), 1151–1169 (2018)
39. Odibat, Z., Baleanu, D.: On a new modification of the erdélyi-kober fractional derivative. Fractal and Fractional **5**(3), 121 (2021)